Appl Microbiol Biotechnol
DOI 10.1007/s00253-013-4725-0

Structural and biochemical characterisation of a NAD^+-dependent alcohol dehydrogenase from *Oenococcus oeni* as a new model molecule for industrial biotechnology applications

Skander Elleuche · Krisztian Fodor · Barbara Klippel · Amélie von der Heyde · Matthias Wilmanns · Garabed Antranikian

Received: 29 November 2012 / Revised: 14 January 2013 / Accepted: 16 January 2013

Abstract Alcohol dehydrogenases are highly diverse enzymes catalysing the interconversion of alcohols and aldehydes or ketones. Due to their versatile specificities, these biocatalysts are of great interest for industrial applications. The *adh3*-gene encoding a group III alcohol dehydrogenase was isolated from the gram-positive bacterium *Oenococcus oeni* and was characterised after expression in the heterologous host *Escherichia coli*. Adh3 has been identified by genome BLASTP analyses using the amino acid sequence of 1,3-propanediol dehydrogenase DhaT from *Klebsiella pneumoniae* and group III alcohol dehydrogenases with known activity towards 1,3-propanediol as target sequences. The recombinant protein was purified in a two-step column chromatography approach. Crystal structure determination and biochemical characterisation confirmed that Adh3 forms a Ni^{2+}-containing homodimer in its active form. Adh3 catalyses the interconversion of ethanol and its corresponding aldehyde acetaldyhyde and is also capable of using other alcoholic compounds as substrates, such as 1,3-propanediol, 1,2-propanediol and 1-propanol. In the presence of Ni^{2+}, activity increases towards 1,3-propanediol and 1,2-propanediol. Adh3 is strictly dependent on NAD^+/NADH, whereas no activity has been observed with $NADP^+$/NADPH as co-factor. The enzyme exhibits a specific activity of 1.1 U/mg using EtOH as substrate with an optimal pH value of 9.0 for ethanol oxidation and 8.0 for aldehyde reduction. Moreover, Adh3 exhibits tolerance to several metal ions and organic solvents, but is completely inhibited in the presence of Zn^{2+}. The present study demonstrates that *O. oeni* is a group III alcohol dehydrogenase with versatile substrate specificity, including Ni^{2+}-dependent activity towards 1,3-propanediol.

Keywords Alcohol dehydrogenase · Zinc · 1,3-propanediol · NAD(H)-dependent · *Oenococcus oeni* · Dimer

Introduction

The interconversion between alcohols and their corresponding aldehydes or ketones is catalysed by alcohol dehydrogenases (ADHs). They are ubiquitous in all organisms, show versatile substrate specificities and can be divided into three non-homologous groups. Zinc-containing long/medium-chain isozymes (group I ADHs) and metal-free short-chain isozymes (group II ADHs) are approximately 350 or 250 amino acids in size, respectively, while the iron-containing ADHs (group III ADHs) exhibit a size of around 385 amino acid residues per subunit (Hernandez-Tobias et al. 2011). It has been shown that $NAD(P)^+$-dependent group III iron-containing ADHs in prokaryotes display broad substrate specificities, with activity towards ethanol, 1,3-propanediol (1,3-PD), 1,2-propanediol (1,2-PD) and butanol. Members of group III ADHs have been identified and characterised from several prokaryotes, such as *Zymomonas mobilis*, *Clostridium acetobutylicum*, *Klebsiella*

Electronic supplementary material The online version of this article (doi:10.1007/s00253-013-4725-0) contains supplementary material, which is available to authorized users.

S. Elleuche · B. Klippel · A. von der Heyde · G. Antranikian (✉)
Institute of Technical Microbiology,
Hamburg University of Technology (TUHH), Kasernenstr. 12,
21073 Hamburg, Germany
e-mail: antranikian@tuhh.de
URL: http://technical-microbiology.de

K. Fodor · M. Wilmanns
European Molecular Biology Laboratory Hamburg,
Notkestraße 85,
22603 Hamburg, Germany

Present Address:
K. Fodor
Department of Biochemistry, Eötvös Loránd University,
Pázmány Péter sétány 1/C,
Budapest 1117, Hungary

Published online: 06 February 2013

pneumoniae, *Escherichia coli*, *Thermotoga lettingae* and *Thermococcus hydrothermalis* (Conway et al. 1987; Walter et al. 1992; Antoine et al. 1999; Sulzenbacher et al. 2004; Montella et al. 2005; Marcal et al. 2009; Chen et al. 2011). Moreover, group III iron-containing ADHs can be further subdivided into several distantly related isozymes based on differences in their primary structure motifs, which have also been shown to display different substrate specificity. These subgroups include butanol dehydrogenases, lactaldehyde:propanediol oxidoreductases and glycerol dehydrogenases. Members of two of these subgroups of group III ADHs have been investigated for their ability to interconvert 1,3-PD: (1) a group of enzymes that share amino acid identity with DhaT from *K. pneumoniae* and (2) a group of YqhD-like isozymes with *E. coli* YqhD being the prototype (Marcal et al. 2009; Jarboe 2011).

1,3-PD is an essential organic compound that is used as a bulk chemical for the production of food additives, drugs, fibres or cosmetics. Moreover, this valuable chemical is mostly known for its use in the production of synthetic polymers such as polyesters, polyethers, and polyurethanes (Xiu and Zeng 2008). In addition to petrochemical routes to synthesise 1,3-PD, fermentative microorganisms of the orders Enterobacteriales and Clostridiales were shown to be capable of producing 1,3-PD in a reductive pathway from glycerol under anaerobic conditions (Daniel et al. 1995; Luers et al. 1997; Ma et al. 2010a; Ashok et al. 2011). This route includes two key enzymes, mainly a glycerol dehydratase (EC 4.2.1.30), which produces 3-hydroxypropionaldehyde (3-HPA) from glycerol and a NAD(P)$^+$-dependent 1,3-PD dehydrogenase (EC 1.1.1.202) to convert 3-HPA into 1,3-PD. The enterococcal species *K. pneumoniae* has been comprehensively investigated for its ability to produce 1,3-PD from glycerol and the *dhaT*-gene has been identified to encode a 1,3-PD dehydrogenase. Substantial research efforts were carried out on strain improvement to produce high levels of 1,3-PD predominately in *E. coli* or *K. pneumoniae* (Cameron et al. 1998; Skraly et al. 1998; Wang et al. 2007; Ma et al. 2010b; Ashok et al. 2011). Moreover, a few native 1,3-PD dehydrogenases and ADHs active towards 1,3-PD were purified from their natural hosts (Johnson and Lin 1987; Talarico et al. 1990; Veiga-da-Cunha and Foster 1992; Luers et al. 1997; Malaoui and Marczak 2000), and some information is currently available on the high-level expression, purification and biochemical characterisation of recombinant 1,3-PD dehydrogenases (Daniel et al. 1995; Fenghuan et al. 2005).

The acidophilic bacterial species *Oenococcus oeni* is the only species in the genus *Oenococcus* beside *O. kitaharae* and belongs to the order of Lactobacillales. This species is of industrial importance because of its high ethanol tolerance and its malolactic fermentation capacity (Mills et al. 2005). In this study, we examined the biochemical properties and the molecular structure of a novel NAD$^+$-dependent group III-ADH Adh3 from *O. oeni*. The crystal structure presents the first group III ADH from a gram-positive bacterium. The biochemical characterisation revealed that this enzyme is capable of catalysing the interconversion of ethanol and acetaldehyde and further short chain compounds, such as 1,3-PD.

Materials and methods

Strains and culture conditions

The gram-positive bacterium *O. oeni* strain DSM20252 was obtained from DSMZ. All cloning experiments were done under standard conditions with the bacterial host strain *E. coli* NovaBlue Singles (Novagen) (Sambrook et al. 2001). *E. coli* strain M15[pREP4] and the expression plasmid pQE-30 (both Qiagen) were used for heterologous expression of the *adh3* gene. Ampicillin (100 μg/ml) and kanamycin (50 μg/ml) were added to Luria Bertani (LB) medium for plasmid maintenance and propagation.

Sequence analysis and gene cloning procedures

The sequence of *adh3* was taken from JGI online database. The public online database NCBI was used to obtain sequences of homologous and related alcohol dehydrogenases (Altschul et al. 1990). Amino acid sequence alignments were performed with selected genes using ClustalX software (Thompson et al. 1997). The online software SignalP 4.0 was used to evaluate the occurrence of signal sequences (Petersen et al. 2011). Gene sequence for primer design was obtained from an open reading frame, which has been annotated as 1,3-propanediol dehydrogenase (ZP_01544043.1) of sequenced strain *O. oeni* ATCC BAA-1163 using primer pair Oo-13PDO-BamHI-f (5′-GGATCCGCAGAGCGTGCATATGATTTTTTG, recognition site for *Bam*HI endonuclease is underlined)/Oo-YqhD-PstI-r (5′-CTGCAGTCATTTTGCATCGTAAGCTTCTTGG, *Pst*I restriction site is underlined). Genomic DNA of strain *O. oeni* DSM20252 was used as template for PCR with Phusion® High-Fidelity DNA-Polymerase (Finzymes) with the following temperature profile: 98 °C for 2 min and 35 cycles of 98 °C for 10 s, 60 °C for 20 s and 72 °C for 30 s and then 72 °C for 7 min for final elongation. The amplicon was ligated into pJET1.2 subcloning vector (Fermentas), and the plasmid was sent to Eurofins MWG Operon (Ebersberg, Germany) for sequence verification. Afterwards, *Bam*HI/*Pst*I digestion fragments were gel-purified using GeneJET™ Gel extraction kit (Fermentas) and cloned into pQE-30 resulting in vector pQE-30-Adh3.

Heterologous expression in *E. coli*

The expression strain *E. coli* M15[pREP4] was transformed with the plasmid pQE-30-Adh3 to produce the His-Adh3 fusion construct. Positive transformants were selected on LB

agar plates supplemented with 100 μg/ml ampicillin and 50 μg/ml kanamycin and were grown in liquid culture medium in 1.2-L fed-batch fermentation approaches. The culture medium was prepared according to Horn et al. (Horn et al. 1996). Expression of *his-adh3* was induced with 2 mM isopropyl-β-D1-thiogalactopyranoside (IPTG) after OD_{600}=50–60 was reached to enable an optimal ratio of soluble protein vs. inclusion bodies in this high-cell-density cultivation. Lower concentrations of IPTG in combination with longer growth periods let to the augmented formation of insoluble protein aggregates. The induced culture was incubated at 37 °C for 2 h and the cells were harvested at an OD_{600}=70–80.

Purification of the recombinant alcohol dehydrogenase Adh3

Proteins were extracted from 5 g wet weight of frozen *E. coli* cells dissolved and thawed in 25 ml of lysis buffer (50 mM NaH_2PO_4, 300 mM NaCl and 10 mM imidazole at pH 8.0) for purification under native conditions. Cell disruption was achieved by using the French press (three times at 2,500 psi; Spin Aminco, Spectronic Instruments). Cell debris was finally precipitated by centrifugation (7,000 rpm) at 4 °C for 30 min. The supernatant was centrifuged again at 13,000 rpm and 4 °C for 30 min. The volume of the cleared lysate was decreased by filtering through a 10.0-kDa molecular weight cut-off Amicon Ultra centrifugal filter unit (Millipore). Purification was achieved using a combination of Ni-NTA affinity chromatography and size exclusion gel filtration with the ÄKTApurifier system (GE Healthcare). The supernatant was loaded onto a Ni-NTA column, which had been equilibrated with lysis buffer. The column was washed with wash buffer (50 mM NaH_2PO_4, 300 mM NaCl and 20 mM imidazole at pH 8.0) at a constant flow rate of 1 ml/min and the protein was finally eluted using elution buffer (50 mM NaH_2PO_4, 300 mM NaCl and 250 mM imidazole at pH 8.0). All active fractions showing a clear band on a sodium dodecyl sulfate-polyacrylamide gel electrophoresis (SDS-PAGE) were pooled and concentrated (Amicon Ultra centrifugal filter unit, Millipore) and dialysed against 50 mM NaH_2PO_4 buffer containing 150 mM NaCl, pH 7.2 (GE Healthcare). The sample was loaded onto a pre-equilibrated HiLoad 16/60 Superdex 200 pg column (GE Healthcare) and the protein was purified using a constant flow rate of 1 ml/min. Native Adh3 was tested for activity and fractions were pooled and concentrated. Finally, the active fractions were dialysed against 50 mM Tris buffer (pH 7.0) and stored at 4 °C. The HiLoad 16/60 Superdex 200 pg column in combination with the HMW Gel Filtration Calibration Kit (GE Healthcare) and a native gradient (4–20 %) Tris-Glycine gel (anamed Elektrophorese GmbH) using the HMW Native Marker Kit (GE Healthcare) was used to estimate the native molecular mass of the purified protein.

SDS-PAGE and Western blotting analyses

Expression of *adh3* in *E. coli* and the purity of the obtained recombinant ADH were visualised by 12 % SDS-PAGE performed in a Mini-PROTEAN Tetra Electrophoresis System (BioRad). Protein transfer to Roti®-PVDF membrane (Roth) was performed with the semi-dry western blotting system (Biometra). The detection was carried out with the His-Tag® AP Western Reagents Kit (Novagen) and His-Tag® Monoclonal Antibody (Novagen) was used as primary and Goat Anti-Mouse FgG AP Conjugate (Novagen) as secondary antibody.

Protein crystallisation and structure determination

Purified Adh3 was concentrated to 80 mg/ml. Crystals were obtained by mixing 2 μl protein with 2 μl reservoir solution, comprising 0.1 M MES (pH 6.5), 16 % (*w*/*w*) PEG20000, and 1 μl 50 mM $CaCl_2$, and submitting to hanging drop vapor diffusion at 20 °C. X-ray data were collected at ID23-2 at ESRF, Grenoble. Data were processed with XDS and scaled with SCALA (Evans 1997; Kabsch 2010). Five percent of the reflections were randomly selected for cross-validation. The structure of the Adh3 was solved by molecular replacement with Phaser using 1,3-propanediol oxidoreductase from *K. pneumoniae* as starting model (PDB entry: 3BFJ), resulting in a log-likelihood gain of 1,296 and a translation function *Z* score of 42 (McCoy et al. 2007; Marcal et al. 2009). REFMAC was used to refine the structure. Manual building and structure analysis were carried out in COOT. The structure quality was assessed with MOLPROBITY (Chen et al. 2010). Programs of the CCP4 package were used for structure manipulation, analysis and validation (Collaborative Computational Project Number 4 1994).

Enzyme assays

The protein concentrations were determined in all experiments by the Bradford method (Bradford 1976). ADH activities were either determined by spectrophotometrically measuring the alcohol-dependent reduction of NAD^+ or the aldehyde-dependent oxidation of NADH at 340 nm in 1 cm pathlength cuvettes using a Cary 300 Bio UV-visible spectrophotometer equipped with a Peltier effect-controlled temperature cuvette holder (Varian, Germany). All experiments were performed in triplicates. The rate of increase (NADH-formation) or decrease (formation of NAD^+) at 340 nm for 1 to 2 min within the first 2 to 6 min, which was in linear range, was recorded. One unit of ADH activity is defined as the amount of enzyme needed to catalyse the reduction or formation of 1 μmol of NAD(H) per min under standard conditions. The standard reaction mixture for alcohol oxidation was composed of 100 mM Tris buffer (pH 9.0), 0.8 mM NAD^+ and an alcoholic substrate (different concentrations depending on the substrate) and was incubated for 10 min at 60 °C. The reaction mixture for aldehyde

reduction contained 100 mM Tris buffer (pH 8.0), 0.8 mM NADH and 10 mM acetaldehyde. Kinetic parameters K_m and v_{max} were obtained using the Solver function of Microsoft Excel.

In vitro enzyme activity was determined for the following substrates: ethanol, 1,3-PD, 1,2-PD, 1-propanol, butanol, methanol, glycerol, β-mercaptoethanol, 2-propanol and acetaldehyde, propanal and butanal. To calculate the pH optimum, reaction measurements were performed at different pH (pH 6–10) with a set of buffers in 50 mM PIPES buffer (pH 6–7) and 100 mM Tris buffer (pH 7–9) and 50 mM Glycerin-NaOH buffer (pH 9–10) with ethanol or acetaldehyde as substrate. Different buffers were tested at the optimal pH to calculate optimal buffer conditions. Temperature optima were calculated for the following substrates: ethanol, 1,3-PD, 1,2-PD and acetaldehyde in range between 10 and 80 °C. Since the solution became slightly turbid at 70 and 80 °C using 1,3-PD and 1,2-PD as substrate, which interfered with the colorimetric determination, end-point measurements were generated with and without substrate and were calculated after centrifugation of the precipitate.

The effect of several compounds at different concentrations on activity was examined after preincubation on ice for 1 h. Residual activity was measured in standard assays including same amount of preincubation compounds. The following metal ions were tested in final concentrations of 1 and 10 mM: Na^+, Ca^{2+}, Ni^{2+}, Mg^{2+} and Zn^{2+}, respectively. The addition of Mn^{2+} and Fe^{2+} interfered with the measurements and could not have been used in the assay. Inhibitory properties of 10 % (*v*/*v*) Tween 20, Tween 80 and Triton X-100, respectively, 0.01 % (*w*/*v*) SDS and 50 % (*v*/*v*) dimethylsulfoxide (DMSO) were tested. The chemical substances guanidine hydrochloride and dithiothreitol (DTT) were applied with a concentration of 10 mM and urea with a concentration of 100 mM. The chelating effect of ethylenediaminetetraacetic acid (EDTA) was tested at concentrations between 0.1 and 200 mM.

Sequence and structural data

Nucleotide sequence data are available in the DDBJ/EMBL/GenBank databases under the accession number HE974350. Structural data are available in the Protein Data Bank/BioMagResBank databases under the accession number RCSB ID code rcsb073248 and PDB ID code 4FR2.

Results

O. oeni adh3 encodes a group III NAD^+-dependent alcohol dehydrogenase

Identification of the open reading frame *adh3* from *O. oeni* was achieved by a genome screening approach for alcohol dehydrogenases with putative activity towards 1,3-PD using the genes *dhaT* from *K. pneumoniae* and *yqhD* from *E. coli* as target sequences (Sulzenbacher et al. 2004; Fenghuan et al. 2005). An annotated, uncharacterised gene encoding a putative 1,3-propanediol dehydrogenase in *O. oeni* ATCC BAA-1163 was found in BLASTP analysis with *K. pneumoniae dhaT* gene as template. The homologous open reading frame could also be found in a TBLASTN analysis in the genome of *O. oeni* PSU-1 using the identified open reading frame of *O. oeni* strain ATCC BAA-1163. In addition, another TBLASTN approach using *yqhD* from *E. coli* as template showed the same open reading frame, although with low sequence identity, indicating that no *yqhD*-homologous gene is encoded within the genome of *O. oeni*. Primer sequences were derived from *O. oeni* ATCC BAA-1163 1,3-PD dehydrogenase sequence to amplify the homologous gene from strain *O. oeni* DSM20252. The *adh3* genes from both strains are highly similar (98.6 % identity at the DNA level and 99.5 % at the protein level) and contain 1,173 bps. The deduced peptide sequence encodes a protein of 390 amino acids with a predicted molecular mass of 42.2 kDa and a theoretical isoelectric point p*I* of 5.23 (Table 1). No putative signal peptide was predicted according to SignalP,

Table 1 Biophysical and biochemical properties of Adh3

Gene (bp)	1,173
Protein (aa)	390
Predicted p*I*	5.23
Predicted molecular weight (kDa)	42.2
EtOH (K_m (mM))[a]	10.4
EtOH (v_{max} (μmol*min^{-1}*mg^{-1}))	4.6
EtOH (K_{cat}/K_m (s^{-1}*mM^{-1}))	0.5
NAD^+ (K_m (mM))[b]	0.05
NAD^+ (v_{max} (μmol*min^{-1}*mg^{-1})	0.2
NAD^+ (K_{cat}/K_m (s^{-1}*mM^{-1}))	4.9
1,3-PD (K_m (mM))[a]	26.7
1,3-PD (v_{max} (μmol*min^{-1}*mg^{-1}))[c]	0.2
1,3-PD (K_{cat}/K_m (s^{-1}*mM^{-1}))	0.01
1,2-PD (K_m (mM))[a]	11.5
1,2-PD (v_{max} (μmol*min^{-1}*mg^{-1})[e]	0.1
1,2-PD (K_{cat}/K_m (s^{-1}*mM^{-1}))	0.01
Acetaldehyde (K_m (mM))[d]	2.6
Acetaldehyde (v_{max} (μmol*min^{-1}*mg^{-1})	2.0
Acetaldehyde (K_{cat}/K_m (s^{-1}*mM^{-1}))	0.9
NADH (K_m (mM))[e]	0.2
NADH (v_{max} (μmol*min^{-1}*mg^{-1})	2.1
NADH (K_{cat}/K_m (s^{-1}*mM^{-1}))	12.9

[a] To calculate K_m of alcoholic compounds, 0.8 mM NAD^+ was used

[b] To calculate K_m (NAD^+), 1 mM EtOH was used

[c] Calculations were done without the addition of $NiCl_2$

[d] To calculate K_m (acetaldehyde), 0.8 mM NADH was used

[e] To calculate K_m (NADH), 2 mM acetaldehyde was used

indicating that *adh3* encodes an intracellular protein. Adh3 shares a high degree of sequence identity on the amino acid level with proteins either annotated as 1,3-PD dehydrogenases or as iron-containing alcohol dehydrogenases from several members of the order Lactobacillales (>70 % amino acid identity), Clostridiales and Enterobacteriales (>50 %). The amino acid sequence of Adh3 shares a sequence identity of 59.2 % in 387 amino acid residues overlap with the characterised homologue DhaT from *K. pneumoniae* and 62.8 % identity to the 1,3-PD dehydrogenase from the gram^{+}-bacterial strain *Clostridium pasteurianum* while only around 20 % sequence identity was found in comparison with established YqhD enzymes from *E. coli* (23.1 % in 350 amino acids overlap) or *K. pneumoniae* (25.1 % in 350 amino acids overlap). A typical group III ADH domain is located in the N-terminal region of the protein and involved in binding the co-factor NAD^{+} with the conserved GGGSxxD co-factor binding site and Asp41 to be the key amino acid residue for co-enzyme specificity (Montella et al. 2005; Ma et al. 2010a; Chen et al. 2011). Moreover, amino acid alignments identified three conserved metal-ion coordinating residues in the C-terminal domain, namely Asp198, His267 and His281, which are common in all 1,3-PD dehydrogenases (Fig. 1). Furthermore, a fourth coordinating residue Gln202 is highly conserved in bacteria of the order Lactobacillales, which is replaced by His202 in Clostridiales and in Enterobacteriales.

Purification of recombinant Adh3

The *adh3* open reading frame was inserted into a pQE-30 vector and a N-terminally His-tagged version was expressed in *E. coli* strain M15[pREP4] as described in "Materials and methods". Gene expression was induced with 2 mM IPTG and the protein was purified from 5 g wet cell weight in a two-step purification protocol (Supplementary Table S1 in the Electronic supplementary material (ESM)). The decrease of specific activity after affinity chromatography is due to the presence of 250 mM imidazole in the elution buffer, which dramatically interfered with enzyme performance. In vitro assays showed that relative activity is reduced down to 32±10.4 % in the presence of 1 mM imidazole and addition of 250 mM resulted in complete inactivity, when pure protein was tested (data not shown). The final specific activity after dialysis of Adh3 is 1.1 U/mg and the enzyme was purified 16-fold and resulted in a yield of 42.3 %. Separation of eluted proteins by SDS-PAGE, coupled to Western blotting analysis using an anti-His antibody revealed a signal with an apparent molecular weight of 43 kDa, which is consistent with the theoretical calculation of the combined molecular weights (43.3 kDa) of the N-terminal RGS-6xHis-tag (1.1 kDa) and Adh3 (42.2 kDa) (Fig. 2).

Adh3 is an active dimer

Members of metal-containing group III ADH can be different with regard to their quarternary structures. While most of the known ADHs are dimeric, the oligomeric state of 1,3-PD from *K. pneumoniae* is decameric (Marcal et al. 2009). To investigate the assembly state of Adh3, size exclusion chromatography and native PAGE analysis were performed. The apparent molecular mass from size exclusion chromatography was 74 kDa±3, indicating that Adh3 forms a dimer, which is in agreement with the native PAGE (Fig. 3). Moreover, a second peak was observed in size exclusion chromatography, which might be due to the formation of aggregates (Fig. 3a). Investigation of this fraction on a native PAGE resulted in a signal that also indicates the formation of aggregates (visible band at >600 kDa) (Fig. 3b). SDS-PAGEs and Western blotting analysis of elution fractions containing dimers or aggregates led to the detection of homogenous single subunits, whose size were consistent with the calculated molecular mass of 43 kDa. However, enzymatic activity tests led to the observation that the dimeric Adh3 is active, while the larger aggregates were inactive (Fig. 3c).

Structure determination

To get a structural overview of the Adh3 enzyme its crystal structure was determined at 3.2 Å resolution (Table 2) (PDB entry, 4FR2). The asymmetric unit contains one enzyme molecule, of which the complete polypeptide chain is visible in the final electron density, except for the N-terminal sequence segment MRGSHHHHHHADGSAER, which also contains the 6xHis-tag, and three residues at the C terminus. Adh3 dimers are formed in the crystals by crystallographic twofold symmetry, with an elongated interaction site at the N-terminal part of the protein (Fig. 4a). The fold of the Adh3 monomer is similar to that of other group III-ADH sequences with known structures. The N-terminal domain (residues 1–186) shows a Rossmann-fold structure, while the C-terminal domain is composed of nine α-helices. The Adh3 structure superimposes well onto similar proteins, such as iron-dependent alcohol dehydrogenase 2 from *Z. mobilis* (root means square deviation (RMSD)=0.83 Å; (PDB entry, 3OX4) (Fig. 4c) or 1,3-propanediol oxidoreductase from *K. pneumoniae* (RMSD=0.83 Å; PDB entry, 3BFJ) (Marcal et al. 2009; Moon et al. 2011).

Careful analysis of the electron density map around the active site showed no sign of a bound co-factor, but the active site metal could have been located. The metal ion was identified as Ni^{2+} by recording X-ray fluorescent spectra from the Adh3 crystals (Fig. 4b; Fig. S1 in the ESM). A predominant peak was observed at 7.43 kEV that is characteristic for Ni^{2+} (KL2 X-ray emission energy for Nickel is 7.46 kEV). While three of the four coordinating amino acids are conserved in group III-ADHs (Asp198, His267 and His281), the third histidine is replaced by

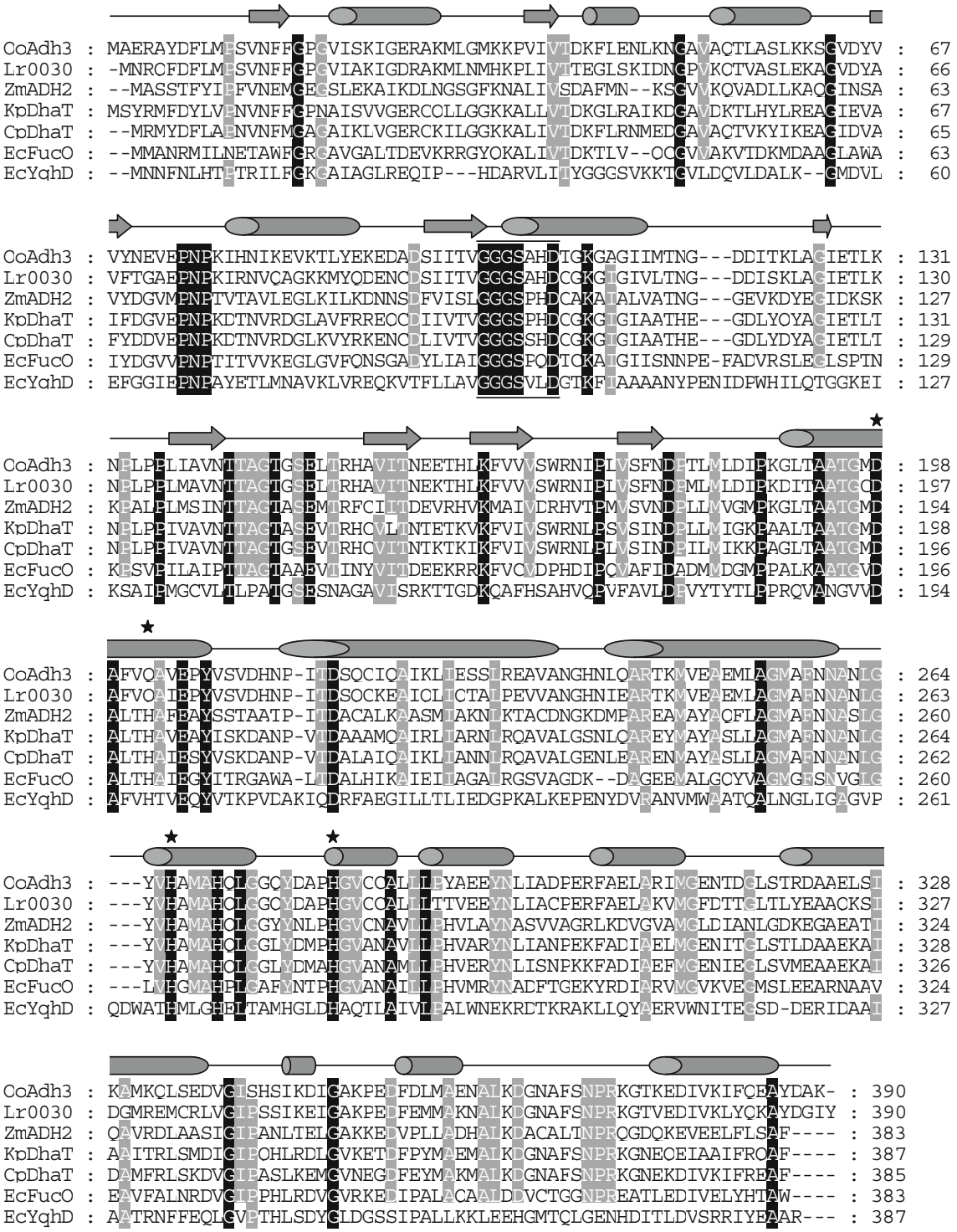

Fig. 1 Multiple sequence alignment of group III alcohol dehydrogenases. Amino acid residues conserved in all sequences are indicated in *white and shaded in black*; residues conserved in at least six sequences are indicated in *white and shaded in grey*. Secondary structure elements of Adh3 are depicted above the aligned sequences. *Barrels* are α-helices and *arrows* are β-sheets. A *black line above and below the alignment* indicates the domain including the GGGSxxD-motif, which is important for co-factor binding. An *asterisk* highlights conserved amino acids important for metal ion coordination. ClustalX alignment was generated using the following sequences: *OoAdh3 O. oeni* Adh3 (this study), *Lr0030 L. reuteri* 13-PDO (5188789), *ZmADH2 Z. mobilis* ADH (BAF76066.1), *KpDhaT K. pneumoniae* DhaT (YP_005956552.1), *CpDhaT C. pasteurianum* DhaT (AF006034), *EcFucO E. coli* FucO (AAA23825.1), *EcYqhD E. coli* YqhD (NP_417484.1)

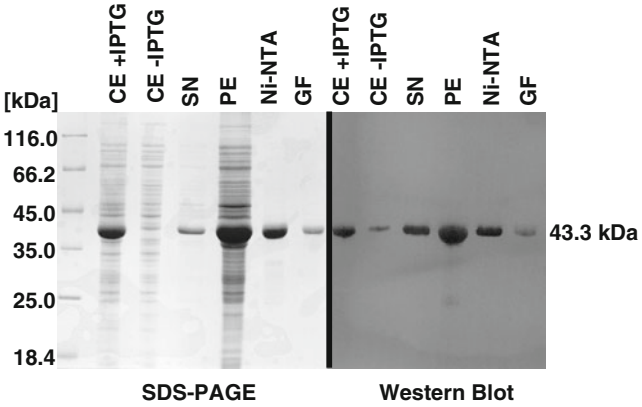

Fig. 2 Expression of His-tagged *O. oeni adh3* gene in *E. coli*. **a** SDS-PAGE of *E. coli* protein extracts harbouring plasmid pQE-30-Adh3 and purification samples. Cells were grown for 2 h at 37 °C after induction with 2 mM IPTG (*+IPTG*) or without the addition of IPTG (*−IPTG*), and total cellular proteins were resolved by SDS-PAGE and visualised by Coomassie Blue staining. Cells were disrupted and the insoluble cell debris (*PE* pellet fraction) was separated by centrifugation from the soluble proteins (*SN* supernatant). His-tagged proteins were purified by affinity chromatography (*Ni-NTA*) and gel filtration (*GF*). **b** Western blotting analysis was used to visualise His-tagged version of Adh3 using anti-His antibody

a glutamine (Gln202) in ADH from gram-positive bacteria of the order Lactobacillales, including Adh3 (Figs. 1 and 4).

Substrate specificity of Adh3

To investigate the substrate promiscuity of recombinant Adh3, the enzyme was studied towards a range of substrates. A specific activity of 1.1 U/mg was measured with EtOH used as the substrate and NAD^+ as the co-factor, while the enzyme showed lower activity towards the primary alcohols 1-propanol (95.8±12.9 % of EtOH activity) and β-mercaptoethanol (32.7±4.2 % of EtOH activity). No activity was detectable by incubation with methanol, 1-butanol, glycerol or 2-propanol. However, Adh3 exhibited a pronounced activity by using diolic compounds as substrates, such as 1,3-PD and 1,2-PD. Interestingly, activity using 1,3-PD as substrate was highly dependent on the addition of $NiCl_2$, while no change in activity was observed using EtOH in a sample with $NiCl_2$. A specific activity of 0.2 U/mg±0.1 was determined with 1,3-PD in combination with NAD^+. The activity was increased up to 0.3 U/mg±0.1 when 1 mM $NiCl_2$ was added to the sample. This effect was

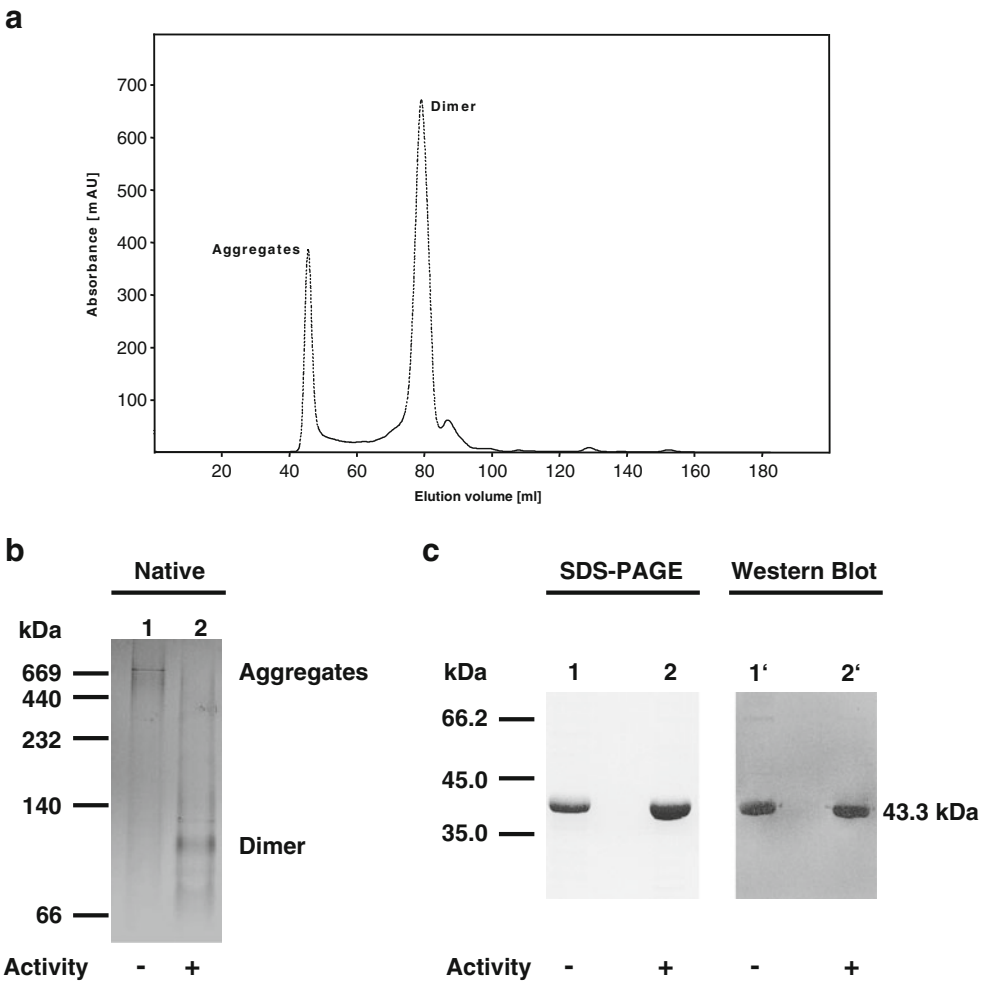

Fig. 3 Determination of dimer and aggregate formation of Adh3 after recombinant expression of the gene in *E. coli*. **a** Size exclusion chromatography of the recombinant *O. oeni* Adh3. Samples from two elution peaks at 46 and 78 ml were used for further investigation. **b** Native PAGE illustrating the formation of aggregates and protein dimers. *Lane 1*, protein aggregates collected from the void volume of size exclusion chromatography. *Lane 2*, sample loaded from 78 ml chromatography elution fraction, indicating the formation of homodimers. **c** Samples of protein aggregates (*lanes 1 and 1'*) and dimer fraction (*lanes 2 and 2'*) were investigated by denaturating SDS-PAGE and Western blotting analysis using His-Tag® Monoclonal Antibody. Activity is indicated below

Table 2 X-ray structure determination

X-ray data collection	
Space group	$P4_32_12$
Cell parameters	$a=b=88.8$ Å, $c=151.03$ Å
Resolution (Å)	99.7–3.2 (3.37–3.20)
Number reflections collected	148,277
Number of unique reflections	10,505
Data completeness (%)	99.6 (100.0)
Mosaicity (deg)	0.24
I/σ (I)	10.8 (1.9)
R_{pim} (%)	4.9 (42.6)
X-ray structure refinement	
R_{work} (%)/R_{free} (%)	27.9/33.4
R.m.s.d. bond length (Å)	0.008
R.m.s.d. bond angles (deg)	1.191
Number of residues	382
Number of solvent molecules	0
Average B factor	88.2
Ramachandran plot	
Favoured	347 (90.81 %)
Allowed	32 (8.41 %)
Outliers	3 (0.78 %)

increased up to 1.5 U/mg±0.2 in the presence of 10 mM $NiCl_2$. Since alcohols undergo oxidation to give aldehydes and ADHs are known to catalyse the interconversion of alcohols and their corresponding aldehydes, the activity of Adh3 towards acetaldehyde was investigated with NADH used as co-factor. The enzyme showed a specific activity of 2.0 U/mg, while no activity was detectable when NADPH was used as co-factor. Lower relative activities were measured using the following substrates: propanal (52.2± 18.5 % of acetaldehyde activity) and butanal (13.7±2.5 % of acetaldehyde activity). Moreover, no activity was observed using $NADP^+$ as co-factor at different concentrations with different alcoholic substrates, indicating that *adh3* encodes an ADH, which uses solely NAD^+ as co-factor.

Biochemical properties of recombinant ADH Adh3

Enzymatic properties as a function of temperature were determined using either alcoholic compounds (EtOH, 1,3-PD or 1,2-PD) or acetaldehyde as substrates (Fig. 5). The activity was measured over a temperature range between 10 and 80 °C with Adh3 showing more than 40 % of activity between 40 and 70 °C with all substrates. Interestingly, the enzyme is not capable of reducing acetaldehyde at 80 °C, while remaining activity for alcohol oxidation was measured. The temperature optimum of *O. oeni* ADH is in a range between 50 to 60 °C (Fig. 5a). Furthermore, Adh3 was incubated for 1 h without substrate at different temperatures to investigate the thermostability of the enzyme (Fig. 5b). Adh3 is stable in 20 mM Tris buffer (pH 7.0) at low temperatures (−20 to 40 °C), but

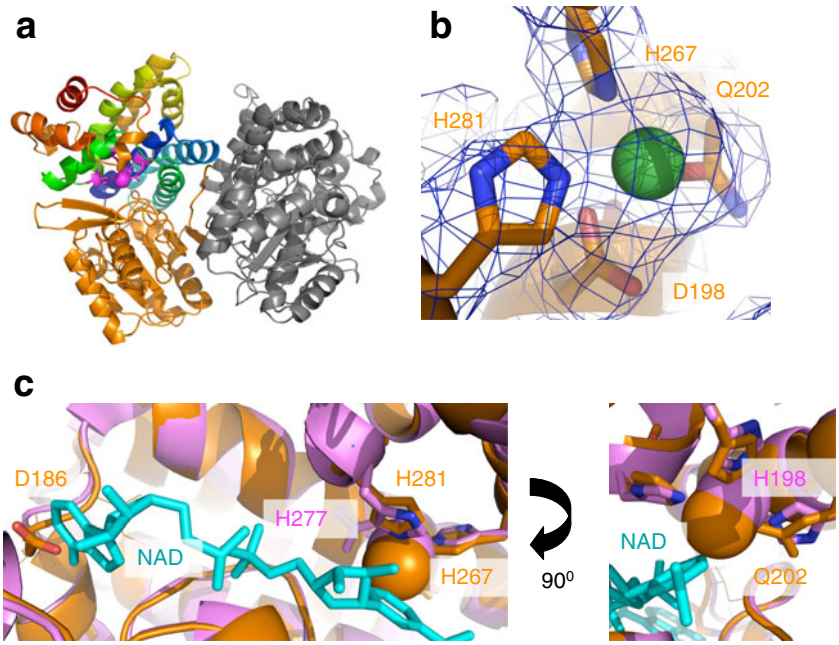

Fig. 4 Structure determination of Adh3. **a** Cartoon representation of the Adh3 dimer. The nine α-helices of the C-terminal domain of the monomer are coloured accordingly, the N-terminal domain is *orange*. The metal co-ordinating site is coloured with *magenta*. The dimer forming symmetry related molecule is coloured *grey*. **b** The Ni^{2+} co-ordination site in the electron density map. The final electron density map is shown at 1.0σ contour level. **c** Superimposition of the *O. oeni* Adh3 (orange) with its *Z. mobilis* counterpart (RCSB ID: 3OX4) (*violet* and *cyan*) in the co-factor binding region. The crystal structure of the *Z. mobilis* protein contains the NAD cofactor (*cyan*), while we were not able to locate electron density for the co-factor in the *O. oeni* Adh3

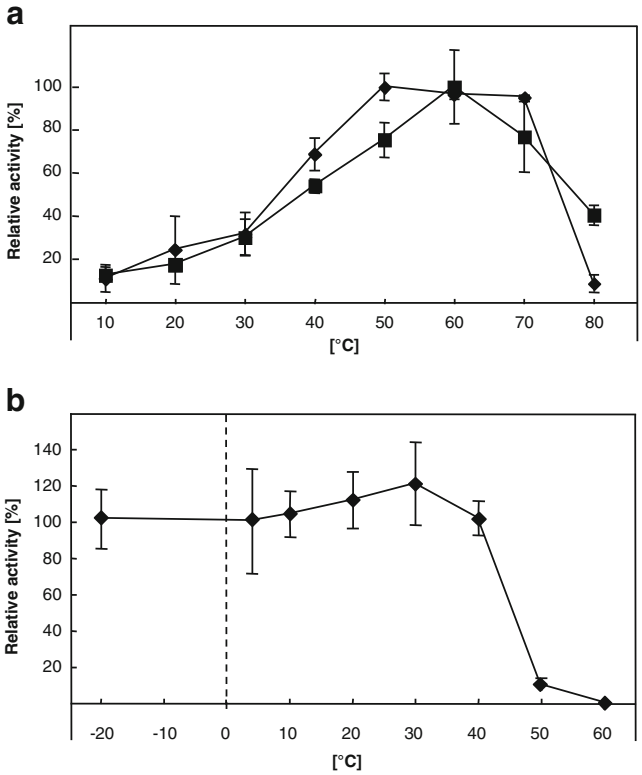

Fig. 5 Influence of temperature on ADH activity and stability. **a** Purified protein was tested at different temperatures under optimal pH conditions with EtOH (*filled squares*) or acetaldehyde (*filled diamonds*) as substrate. **b** Enzyme stability was examined after incubation at different temperatures for 60 min using ethanol as substrate. Enzymatic reactions were carried out as described in "Material and methods"

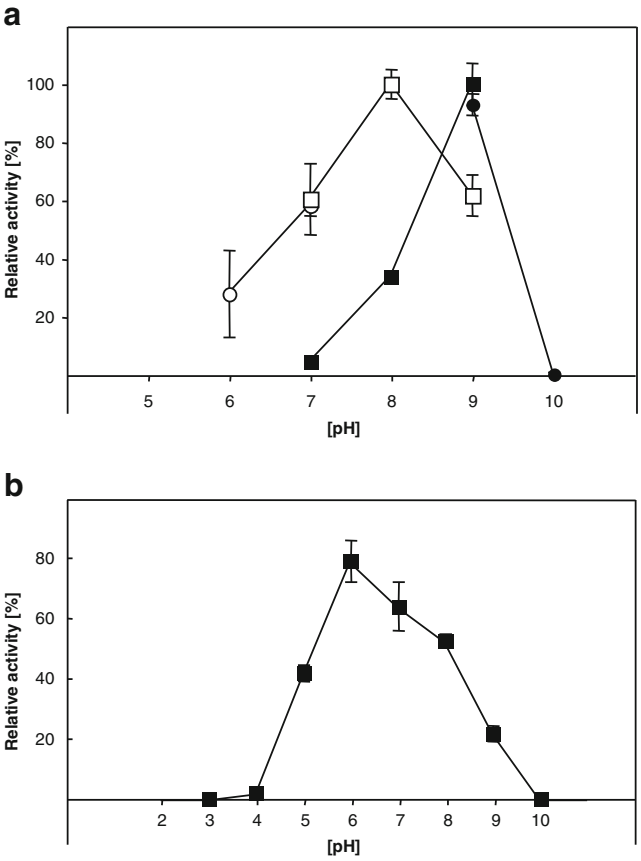

Fig. 6 Influence of pH on the activity of Adh3 from *O. oeni*. **a** For the determination of the pH optimum, Adh3 was incubated in Tris (*filled squares*) and GlyNaOH buffer (*filled circles*) when ethanol was used as substrate. To investigate the pH optimum for acetaldehyde reduction, activity of Adh3 was tested in Tris (*open squares*) and PIPES buffer (*open circles*). **b** Enzyme stability was examined after incubation for 60 min in universal buffer at different pH using ethanol as substrate (Britton and Robinson 1931). Enzymatic reactions were carried out as described in "Material and methods"

becomes inactive after incubation for 60 min at temperatures higher than 50 °C. Freezing the protein in buffer without antifreeze components resulted in a complete loss of activity after 3 h at −80 °C and after 2 days at −20 °C. Lyophilisation did also not improve storage time (data not shown).

The optimal pH was shown to be pH 9.0 in 100 mM Tris buffer using alcoholic compounds as substrates (EtOH, 1,3-PD or 1,2-PD), while an optimal pH of 8.0 was determined with acetaldehyde as substrate in 100 mM Tris buffer (Fig. 6a). It was observed that the activity was highly dependent on the applied buffer system (Fig. S2 in the ESM). Due to the influence of different buffer systems on the enzymatic activity, universal buffer (pH 2–11) was used to measure the pH-dependent stability (Fig. 6b). Accordingly, Adh3 was most stable at pH 6 to 7. The apparent kinetic parameters were determined at optimal pH 9.0 and 60 °C for alcoholic substrates and at pH 8.0 for acetaldehyde (Table 1).

Inhibiting and activating effects of metal ions and reagents

Activating and inhibiting effects of mono- and divalent cations were investigated for recombinant ADH from *O. oeni*. Incubation at low concentrations of NaCl (1 and 10 mM) and at 10 mM of $MgCl_2$ increased the activity of Adh3, while $ZnCl_2$ completely inhibited enzymatic activity (Fig. 7a). Moreover, several chemical compounds and detergents were tested (Fig. 7b). Tween 20 completely blocked the enzyme at a concentration of 10 %, while Tween 80 and Triton X-100 had opposite effects and increased Adh3 activity. Moreover, 50 % of the organic solvent DMSO completely blocked catalytic activity. The chaotropic salt guanidine hydrochloride and DTT only had limited effects on catalytic activity. The detergent SDS reduced catalytic activity down to 72±13 % at a concentration of 0.01 % (*w*/*v*), while a concentration of 0.1 % (*w*/*v*) SDS blocked the catalytic activity without preincubation of the enzyme (data not shown). Since Adh3 is coordinating a metal ion in its catalytic region, the inhibitory effect of the chelating agent EDTA was tested experimentally (Fig. 7c). No influence was detected by using EDTA concentrations up to 10 mM, while activity was reduced to 32±9.9 % with 50 mM

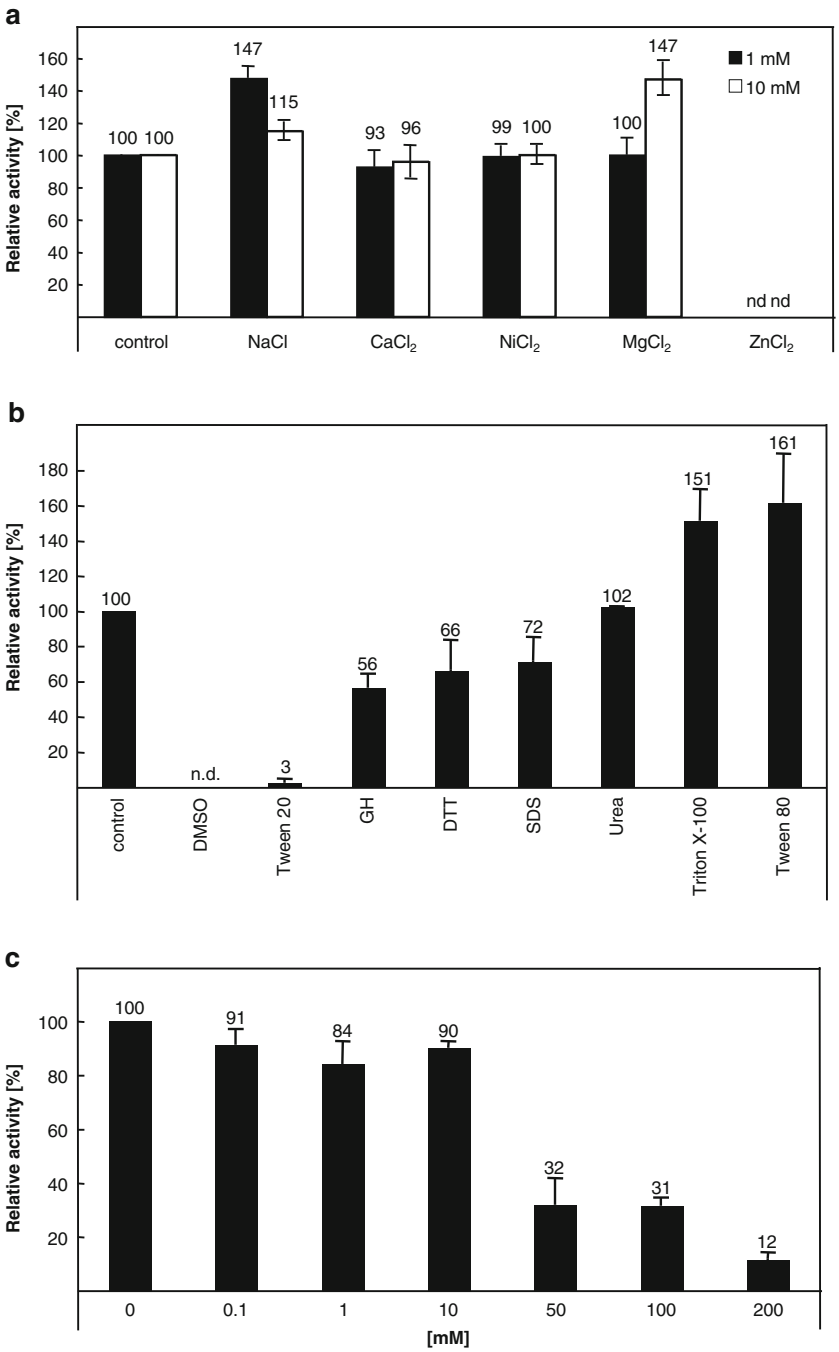

Fig. 7 Influence of various chemical compounds on the catalytic activity of Adh3. **a** Metal ions were tested for activating or inhibitory effects on Adh3 from *O. oeni*. Adh3 was incubated for 60 min on ice in the presence of various metal ions. For examination of the residual activity, preincubation mixture was tested in standard assay mixtures including equal concentrations of metal ions. **b** Effects of putative ADH inhibitors and organic solvents were examined. The assay was performed as described for metal ions. *GH* guanidine hydrochloride. **c** Inhibition of enzymatic activity by chelation. Adh3 was incubated in the presence of EDTA at different concentrations to investigate inhibitory effects. *nd* not determined

EDTA used in the sample. Residual activity of 12±2.5 % was obtained by incubation with 200 mM of EDTA for 1 h.

Discussion

Due to their multiple applications in industrial processes, ADHs have gained considerable interest. In this context biocatalysts applicable for the production of valuable fine chemicals are of tremendous interest to replace chemical processing routes. Our data suggest that Adh3 from *O. oeni* can be a candidate because of its activity to process several short chain alcoholic and aldehyde substrates.

Two main subgroups of group III ADHs have been investigated with regard to activity towards 1,3-PD. The group of enzymes that share amino acid identity with DhaT from *K. pneumoniae* and the group of YqhD isozymes with *E. coli* YqhD being the prototype (Johnson and Lin 1987; Jarboe 2011). The catalytic efficiency of *E. coli* YqhD in converting 3-HPA into 1,3-PD is lower than that of "real" 1,3-PD dehydrogenases, such as DhaT from *K. pneumoniae*. Although the genomes of several bacterial species exhibit

homologues of both or even more types of group III ADHs, the genome of *O. oeni* encodes for a single putative group III ADH, which could be identified by BLASTP-analyses with DhaT or YqhD used as a template. Recently, two 1,3-PD dehydrogenases were investigated in another gram-positive bacterium *Lactobacillus reuteri*. The open reading frame lr_1734 is related to Adh3 (76.4 % identity on the amino acid level) and encodes a protein that is crucial for 1,3-PD production under physiological conditions, while lr-0030 belongs to another group of 1,3-PD dehydrogenase encoding genes, indicating that detailed investigation including knockout- or activity-screening may open the road to other unknown ADHs with potential in 1,3-PD processing (Stevens et al. 2011).

The structure of the dimeric enzyme Adh3 resembles 1,3-PD dehydrogenase DhaT from *K. pneumoniae* and alcohol dehydrogenase 2 from *Z. mobilis* and can be clearly assigned to the family of metal ion-containing group III ADHs. While typical group III ADHs such as *E. coli* FucO or TM0920 from *Thermotoga maritima* are mainly catalytic dimers, the dimers of DhaT from *K. pneumoniae* were shown to form a star-like decameric structure composed of five dimers, which was not observed for Adh3 (Marcal et al. 2009) (Fig. S3 in the ESM). Interestingly, pH-dependent formation of active dimers and inactive tetramers was observed for a group III ADH from *T. hydrothermalis* while Adh3 formed inactive aggregates and active dimeric structures (Antoine et al. 1999). The unit cell of the Adh3 crystal contained a single monomer; therefore no putative structural differences between the subunits of the dimer could have been observed for this enzyme. The three-dimensional structure of Adh3 contains a conserved structural model called the Rossmann fold, composed of α-helices surrounding a conserved arrangement of six parallel β-sheets. The highly conserved amino acid residues, which were shown to be important for metal-ion coordination in *K. pneumoniae* DhaT and other ADHs derived from gram-negative bacteria, are conserved in Adh3. In contrast to DhaT, *Z. mobilis* ZmADH2 and *E. coli* FucO, which contain Fe^{2+} ion, Ni^{2+} was identified in the structure of Adh3 (Fig. S1 in the ESM). It is important to note, that although the solution used for crystallisation did not contain nickel, the possibility that the observed nickel in the active site is an artefact due to contamination during recombinant protein expression or purification cannot be excluded. In good agreement with *K. pneumoniae* DhaT, high concentrations of EDTA were necessary to obtain an inhibition. Adh3 activity is reduced to 32 % by incubation with 50 mM EDTA, which is comparable to 50 % residual activity of DhaT in the presence of 50 mM EDTA (Marcal et al. 2009). The highly conserved Asp41 was deduced to be the key amino acid residue responsible for the NAD^+ specificity in *K. pneumoniae* DhaT and in *E. coli* FucO (Montella et al. 2005; Ma et al. 2010a). The structure of Adh3 reveals that Asp41 is located in the same position, even in the absence of the co-factor. However, the loop containing Asp186 is displaced towards the co-factor interaction site and should probably slightly move away upon co-factor binding (Fig. 4c).

Biochemical investigations revealed that Adh3 from *O. oeni* displayed a broad pH-spectrum and catalysed the oxidation of several alcoholic and the reduction of aldehyde compounds. While activity towards several primary alcohols was detected, the enzyme was not capable of oxidising 2-propanol. Adh3 displayed an unusual temperature optimum between 50 °C and 60 °C, which is near the optimum of another ADH from *O. oeni* strain CECT4730 (Meng and Xu 2010). This specific enzyme was shown to be highly active towards 2-octanone and displayed optimal activity at a temperature of 45 °C, while isozymes from the thermophilic Archaea *T. hydrothermalis* and from *Thermococcus* strain ES1 exhibited temperature optima of 80 °C and around 95 °C, respectively (Antoine et al. 1999; Ying et al. 2009; Meng and Xu 2010). Moreover, different pH optima for reduction and oxidation reactions are typical for various ADHs (Antoine et al. 1999; Kosjek et al. 2004; Ying et al. 2009; Chen et al. 2011; Timpson et al. 2013).

Due to the higher affinity to ethanol in comparison to 1,3-PD and the fact that no open reading frames encoding putative glycerol dehydratases or their activating proteins related to the *K. pneumoniae* or *C. butyricum* isozymes could be found by genome analyses, we assume that *O. oeni* is most probably not able to produce 1,3-PD under natural conditions. The enzyme Adh3 might be involved in the important regulation of ethanol tolerance in *O. oeni*, but this speculation needs to be proven through detailed investigation. The physiological role of DhaT from *K. pneumoniae* has been speculated to be the regeneration of NAD^+, which is needed for the NAD^+-linked glycerol degradation in the oxidative pathway (Ashok et al. 2011). In comparison to Adh3 (K_m=26.7 mM), kinetic analyses revealed a K_m of 16.7 mM for *K. pneumoniae* 1,3-PD dehydrogenase DhaT using 1,3-PD as substrate (Marcal et al. 2009). In addition to 1,3-PD, the propanediol 1,2-PD is also of industrial interest as a de-icer or feedstock in the production of polyesters or speciality chemicals (Bennett and San 2001). Adh3 catalyses 1,2-PD oxidation. It displayed a K_m of 11.5 mM. Under natural conditions, 1,2-PD is produced by the activity of a NADH-dependent 1,2-PD oxidoreductase in several bacteria and yeasts. This enzyme catalyses the formation of 1,2-PD by reduction of the precursor molecule lactaldehyde. Moreover, an unspecific ADH with a K_m of 166 mM for 1,2-PD and 0.48 mM for ethanol from *Desulfovibrio* strain HDv has been described to be responsible for growth on 1,2-PD (Hensgens et al. 1995). Since Adh3 displays activity towards 1,2-PD and is related to FucO (1,2-PD

oxidoreductase) from *E. coli* (37.9 % identity in 385 amino acid residues overlap), this specific enzyme might be a potential candidate for applications in processing 1,2-PD as well.

Nowadays, there is a considerable interest in the environmental friendly production of chemicals, which can compete with petrochemical routes. Moreover, ADHs are of tremendous interest with regard towards the production of enantioselective products. A detailed investigation of Adh3 in the future will answer the question if this protein is a potential candidate for the production of chiral fine chemicals for industrial applications. Nevertheless, there are still some remaining barriers to overcome. In this context, several strategies were used to improve the production level of chemical compounds, such as combination of genes from different strains in a heterologous organism, purification of enzymes from natural hosts, improvement of well-established and multi-mutated production organisms, generation of an elegant expression of artificial bicistronic operons or fusion (Wang et al. 2007; Chatzifragkou et al. 2011; Rujanonon et al. 2011; Qi et al. 2012). To guarantee ongoing success, there is a need for novel, well-characterised, functional and easy-to-handle ADH candidates, with side activity towards 1,3-PD to pave the way for future highly productive strains.

Acknowledgments The authors thank Henning Piascheck for his help with the fermentation experiments. X-ray data collection was performed on the ID23-2 beamline at the European Synchrotron Radiation Facility (ESRF), Grenoble, France. We are grateful to Cristoph Müller-Dickmann at ESRF for providing assistance in using beamline ID23-2. This work was funded by the Excellence Cluster in the Excellence Initative by the State of Hamburg "Fundamentals of Synthetic Biological Systems (SynBio)". The work was also supported by the Hungarian National Scientific Research Foundation (OTKA) grant PD104365.

References

Altschul SF, Gish W, Miller W, Myers EW, Lipman DJ (1990) Basic local alignment search tool. J Mol Biol 215:403–410

Antoine E, Rolland JL, Raffin JP, Dietrich J (1999) Cloning and overexpression in *Escherichia coli* of the gene encoding NADPH group III alcohol dehydrogenase from *Thermococcus hydrothermalis*. Characterization and comparison of the native and the recombinant enzymes. Eur J Biochem 264:880–889

Ashok S, Raj SM, Rathnasingh C, Park S (2011) Development of recombinant *Klebsiella pneumoniae dhaT* strain for the co-production of 3-hydroxypropionic acid and 1,3-propanediol from glycerol. Appl Microbiol Biotechnol 90:1253–1265

Bennett GN, San KY (2001) Microbial formation, biotechnological production and applications of 1,2-propanediol. Appl Microbiol Biotechnol 55:1–9

Bradford MM (1976) A rapid and sensitive method for the quantitation of microgram quantities of protein utilizing the principle of protein-dye binding. Anal Biochem 72:248–254

Britton HTK, Robinson RA (1931) CXCVIII.-Universal buffer solutions and the dissociation constant of veronal. J Chem Soc 458:1456–1462

Cameron DC, Altaras NE, Hoffman ML, Shaw AJ (1998) Metabolic engineering of propanediol pathways. Biotechnol Prog 14:116–125

Chatzifragkou A, Papanikolaou S, Dietz D, Doulgeraki AI, Nychas GJ, Zeng AP (2011) Production of 1,3-propanediol by *Clostridium butyricum* growing on biodiesel-derived crude glycerol through a non-sterilized fermentation process. Appl Microbiol Biotechnol 91:101–112

Chen R, Yin X, Yu C, Wang Q, Zhan X, Xie T (2011) Characterization of the recombinant group 3 alcohol dehydrogenase from *Thermotoga lettingae* TMO. Afr J of Microbiol Res 5:4004–4012

Chen VB, Arendall WB 3rd, Headd JJ, Keedy DA, Immormino RM, Kapral GJ, Murray LW, Richardson JS, Richardson DC (2010) MolProbity: all-atom structure validation for macromolecular crystallography. Acta Crystallogr D: Biol Crystallogr 66:12–21

Collaborative Computational Project 4 (1994) The CCP4 suite: programs for protein crystallography. Acta Crystallogr D: Biol Crystallogr 50:760–763

Conway T, Sewell GW, Osman YA, Ingram LO (1987) Cloning and sequencing of the alcohol dehydrogenase II gene from *Zymomonas mobilis*. J Bacteriol 169:2591–2597

Daniel R, Boenigk R, Gottschalk G (1995) Purification of 1,3-propanediol dehydrogenase from *Citrobacter freundii* and cloning, sequencing, and overexpression of the corresponding gene in *Escherichia coli*. J Bacteriol 177:2151–2156

Evans PR (1997) SCALA. Joint CCP4 and ESF-EAMBC. Newslon Protein Crystallogr 33:22–24

Fenghuan W, Huijin Q, He H, Tan T (2005) High-level expression of the 1,3-propanediol oxidoreductase from *Klebsiella pneumoniae* in *Escherichia coli*. Mol Biotechnol 31:211–219

Hensgens CMH, Jansen M, Nienhuis-Kuiper ME, Boekema EJ, Van Breemen JFL, Hansen TA (1995) Purification and characterization of an alcohol dehydrogenase from 1,2-propanediol-grown *Desulfovibrio* strain HDv. Arch Microbiol 164:265–270

Hernandez-Tobias A, Julian-Sanchez A, Pina E, Riveros-Rosas H (2011) Natural alcohol exposure: is ethanol the main substrate for alcohol dehydrogenases in animals? Chem Biol Interact 191:14–25

Horn U, Strittmatter W, Krebber A, Knupfer U, Kujau M, Wenderoth R, Muller K, Matzku S, Pluckthun A, Riesenberg D (1996) High volumetric yields of functional dimeric miniantibodies in *Escherichia coli*, using an optimized expression vector and high-cell-density fermentation under non-limited growth conditions. Appl Microbiol Biotechnol 46:524–532

Jarboe LR (2011) YqhD: a broad-substrate range aldehyde reductase with various applications in production of biorenewable fuels and chemicals. Appl Microbiol Biotechnol 89:249–257

Johnson EA, Lin EC (1987) *Klebsiella pneumoniae* 1,3-propanediol: NAD^+ oxidoreductase. J Bacteriol 169:2050–2054

Kabsch W (2010) Xds. Acta Crystallogr D: Biol Crystallogr 66:125–132

Kosjek B, Stampfer W, Pogorevc M, Goessler W, Faber K, Kroutil W (2004) Purification and characterization of a chemotolerant alcohol dehydrogenase applicable to coupled redox reactions. Biotechnol Bioeng 86:55–62

Luers F, Seyfried M, Daniel R, Gottschalk G (1997) Glycerol conversion to 1,3-propanediol by *Clostridium pasteurianum*: cloning and expression of the gene encoding 1,3-propanediol dehydrogenase. FEMS Microbiol Lett 154:337–345

Ma C, Zhang L, Dai J, Xiu Z (2010a) Relaxing the coenzyme specificity of 1,3-propanediol oxidoreductase from *Klebsiella pneumoniae* by rational design. J Biotechnol 146:173–178

Ma Z, Rao Z, Zhuge B, Fang H, Liao X, Zhuge J (2010b) Construction of a novel expression system in *Klebsiella pneumoniae* and its application for 1,3-propanediol production. Appl Biochem Biotechnol 162:399–407

Malaoui H, Marczak R (2000) Purification and characterization of the 1,3-propanediol dehydrogenase of *Clostridium butyricum* E5. Enzyme Microb Technol 27:399–405

Marcal D, Rego AT, Carrondo MA, Enguita FJ (2009) 1,3-propanediol dehydrogenase from *Klebsiella pneumoniae*: decameric

quaternary structure and possible subunit cooperativity. J Bacteriol 191:1143–1151

McCoy AJ, Grosse-Kunstleve RW, Adams PD, Winn MD, Storoni LC, Read RJ (2007) Phaser crystallographic software. J Appl Crystallogr 40:658–674

Meng F, Xu Y (2010) Purification and characterization of an anti-Prelog alcohol dehydrogenase from *Oenococcus oeni* that reduces 2-octanone to (R)-2-octanol. Biotechnol Lett 32:533–537

Mills DA, Rawsthorne H, Parker C, Tamir D, Makarova K (2005) Genomic analysis of *Oenococcus oeni* PSU-1 and its relevance to winemaking. FEMS Microbiol Rev 29:465–475

Montella C, Bellsolell L, Perez-Luque R, Badia J, Baldoma L, Coll M, Aguilar J (2005) Crystal structure of an iron-dependent group III dehydrogenase that interconverts L-lactaldehyde and L-1,2-propanediol in *Escherichia coli*. J Bacteriol 187:4957–4966

Moon JH, Lee HJ, Park SY, Song JM, Park MY, Park HM, Sun J, Park JH, Kim BY, Kim JS (2011) Structures of iron-dependent alcohol dehydrogenase 2 from *Zymomonas mobilis* ZM4 with and without NAD + cofactor. J Mol Biol 407:413–424

Petersen TN, Brunak S, von Heijne G, Nielsen H (2011) SignalP 4.0: discriminating signal peptides from transmembrane regions. Nat Methods 8:785–786

Qi X, Guo Q, Wei Y, Xu H, Huang R (2012) Enhancement of pH stability and activity of glycerol dehydratase from *Klebsiella pneumoniae* by rational design. Biotechnol Lett 34:339–346

Rujanonon R, Praertsan P, Phongdara A, Panrat T, Sun J, Rappert S, Zeng AP (2011) Construction of recombinant *E. coli* expressing fusion protein to produce 1,3-propanediol. Int J of Biol and Med Sci 1:26–32

Sambrook J, Fritsch E, Maniatis T (2001) Molecular cloning: a laboratory manual, 3rd edn. Cold Spring Harbor Laboratory Press, Cold Spring Harbor

Skraly FA, Lytle BL, Cameron DC (1998) Construction and characterization of a 1,3-propanediol operon. Appl Environ Microbiol 64:98–105

Stevens MJ, Vollenweider S, Meile L, Lacroix C (2011) 1,3-propanediol dehydrogenases in *Lactobacillus reuteri*: impact on central metabolism and 3-hydroxypropionaldehyde production. Microb Cell Fact 10:61

Sulzenbacher G, Alvarez K, Van Den Heuvel RH, Versluis C, Spinelli S, Campanacci V, Valencia C, Cambillau C, Eklund H, Tegoni M (2004) Crystal structure of *E. coli* alcohol dehydrogenase YqhD: evidence of a covalently modified NADP coenzyme. J Mol Biol 342:489–502

Talarico TL, Axelsson LT, Novotny J, Fiuzat M, Dobrogosz WJ (1990) Utilization of glycerol as a hydrogen acceptor by *Lactobacillus reuteri*: purification of 1,3-propanediol:NAD oxidoreductase. Appl Environ Microbiol 56:943–948

Thompson JD, Gibson TJ, Plewniak F, Jeanmougin F, Higgins DG (1997) The CLUSTAL_X windows interface: flexible strategies for multiple sequence alignment aided by quality analysis tools. Nucleic Acids Res 25:4876–4882

Timpson LM, Liliensiek AK, Alsafadi D, Cassidy J, Sharkey MA, Liddell S, Allers T, Paradisi F (2013) A comparison of two novel alcohol dehydrogenase enzymes (ADH1 and ADH2) from the extreme halophile *Haloferax volcanii*. Appl Microbiol Biotechnol 97:195–203

Veiga-da-Cunha M, Foster MA (1992) 1,3-propanediol:NAD^+ oxidoreductases of *Lactobacillus brevis* and *Lactobacillus buchneri*. Appl Environ Microbiol 58:2005–2010

Walter KA, Bennett GN, Papoutsakis ET (1992) Molecular characterization of two *Clostridium acetobutylicum* ATCC 824 butanol dehydrogenase isozyme genes. J Bacteriol 174:7149–7158

Wang F, Qu H, Zhang D, Tian P, Tan T (2007) Production of 1,3-propanediol from glycerol by recombinant *E. coli* using incompatible plasmids system. Mol Biotechnol 37:112–119

Xiu ZL, Zeng AP (2008) Present state and perspective of downstream processing of biologically produced 1,3-propanediol and 2,3-butanediol. Appl Microbiol Biotechnol 78:917–926

Ying X, Grunden AM, Nie L, Adams MW, Ma K (2009) Molecular characterization of the recombinant iron-containing alcohol dehydrogenase from the hyperthermophilic Archaeon, *Thermococcus* strain ES1. Extremophiles 13:299–311